

## Thermodynamic analyses of the orthorhombic-to-tetragonal phase transition in $\text{Pr}_{2-x}\text{Nd}_x\text{NiO}_{4+\delta}$ under controlled oxygen partial pressures

Eiki Niwa<sup>1</sup>, Tsubasa Sato<sup>2</sup>, Takuya Hashimoto<sup>2</sup>

<sup>1</sup> Department of Chemistry for Materials, Graduate School of Engineering, Mie University, Tsu, Mie, 514-8507, Japan

<sup>2</sup> Department of Physics, College of Humanities and Sciences, Nihon University, Setagaya-ku, Tokyo, 156-8550, Japan

### Supporting Information

**Figure S1.** Rietveld patterns of  $\text{Pr}_2\text{NiO}_{4+\delta}$  by XRD using the computer program Z-code [1, 2]. Crystal structure models are (a) orthorhombic  $Fmmm$  and (b) mixed phase of  $Fmmm$  and monoclinic  $F112/m$ . The obtained and calculated patterns and difference plots are shown by red mark, light blue, and dark blue lines, respectively. Bragg peak positions are estimated from the obtained lattice constants. Green and orange tick marks indicate the Bragg peak positions of  $Fmmm$  and  $F112/m$ , respectively.

**Figure S2.** DSC curves of  $\text{PrNdNiO}_{4+\delta}$  around the phase transition temperatures under various  $P(\text{O}_2)$  during (a) heating and (b) cooling.

**Figure S3.** DSC curves of  $\text{Pr}_{0.5}\text{Nd}_{1.5}\text{NiO}_{4+\delta}$  around the phase transition temperatures under various  $P(\text{O}_2)$  during (a) heating and (b) cooling.

**Figure S4.** TG curves of  $\text{PrNdNiO}_{4+\delta}$  around the phase transition temperatures under various  $P(\text{O}_2)$  during (a) heating and (b) cooling.

**Figure S5.** TG curves of  $\text{Pr}_{0.5}\text{Nd}_{1.5}\text{NiO}_{4+\delta}$  around the phase transition temperatures under various  $P(\text{O}_2)$  during (a) heating and (b) cooling.

**Figure S6.** Compositional dependence of oxygen content,  $\delta$ , of  $\text{Pr}_{2-x}\text{Nd}_x\text{NiO}_{4+\delta}$  at the beginning of the phase transition during heating under  $P(\text{O}_2)$  of  $1.0 \times 10^{-2}$  bar. The values in parentheses show the phase transition temperatures.

**Figure S7. XRD pattern of  $\text{Pr}_2\text{NiO}_{4+\delta}$  after the decomposition reaction under 2% $\text{H}_2/\text{N}_2$ . For reference, XRD patterns of  $\text{Pr}_2\text{O}_3$  and Ni are also shown in this figure [3, 4].**

**Figure S8. Compositional dependence of the phase transition temperatures,  $T_p$ , of  $\text{Pr}_{2-x}\text{Nd}_x\text{NiO}_{4+\delta}$  in air ( $P(\text{O}_2) = 0.205$  bar), estimated using  $\Delta S^\circ$  and  $\Delta H^\circ$  obtained in this work and measured with DTA [5].**

**Table S1 (a) Lattice constants and (b) reliability factors for the XRD data of  $\text{Pr}_2\text{NiO}_{4+\delta}$  by the Rietveld analysis with two kinds of models; a single phase of the orthorhombic  $Fmmm$  (Model 1) and the mixed phase of  $Fmmm$  and  $F122/m$  (Model 2), as shown in Figures S1 (a) and (b).**

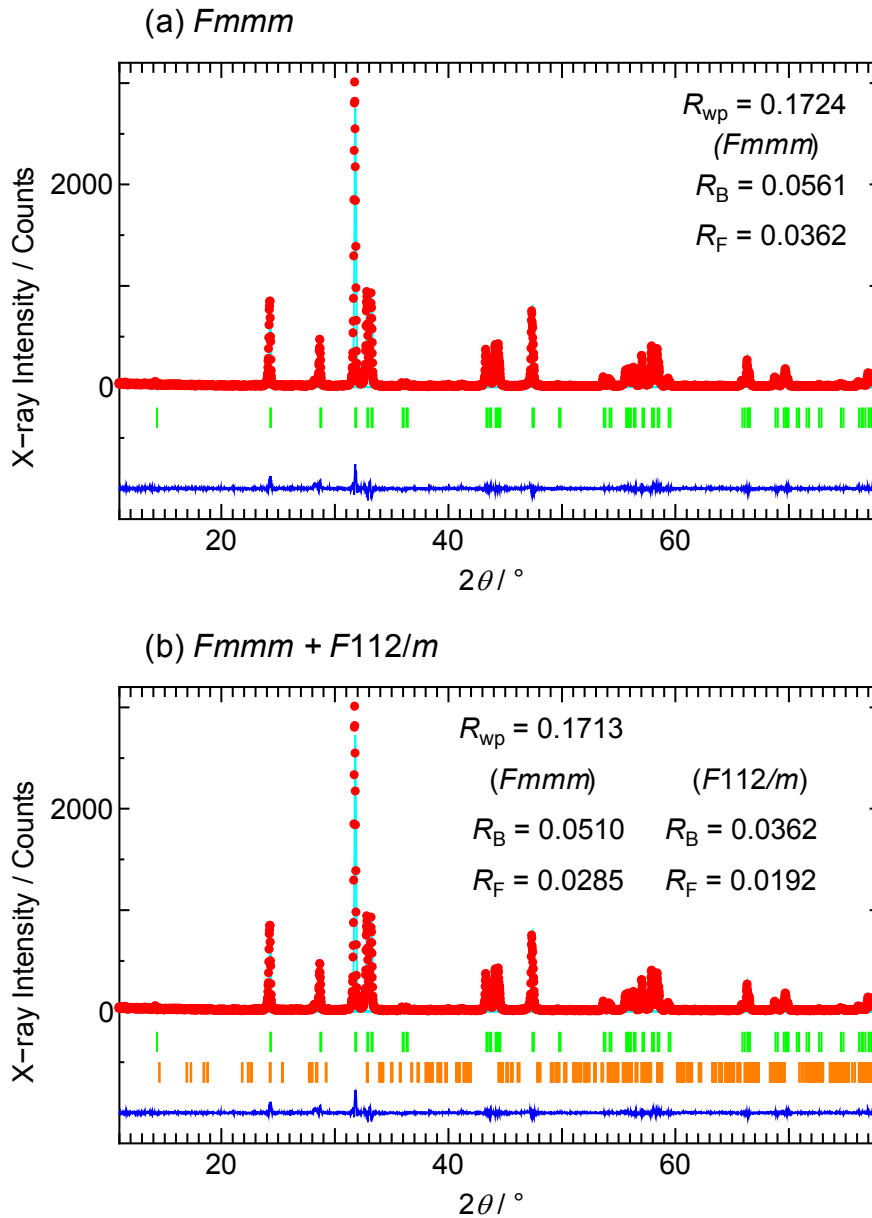


Figure S1. Rietveld patterns of  $\text{Pr}_2\text{NiO}_{4+\delta}$  by XRD using the computer program Z-code [1, 2]. Crystal structure models are (a) orthorhombic *Fmmm* and (b) mixed phase of *Fmmm* and monoclinic *F112/m*. The obtained and calculated patterns and difference plots are shown by red mark, light blue, and dark blue lines, respectively. Bragg peak positions are estimated from the obtained lattice constants. Green and orange tick marks indicate the Bragg peak positions of *Fmmm* and *F112/m*, respectively.

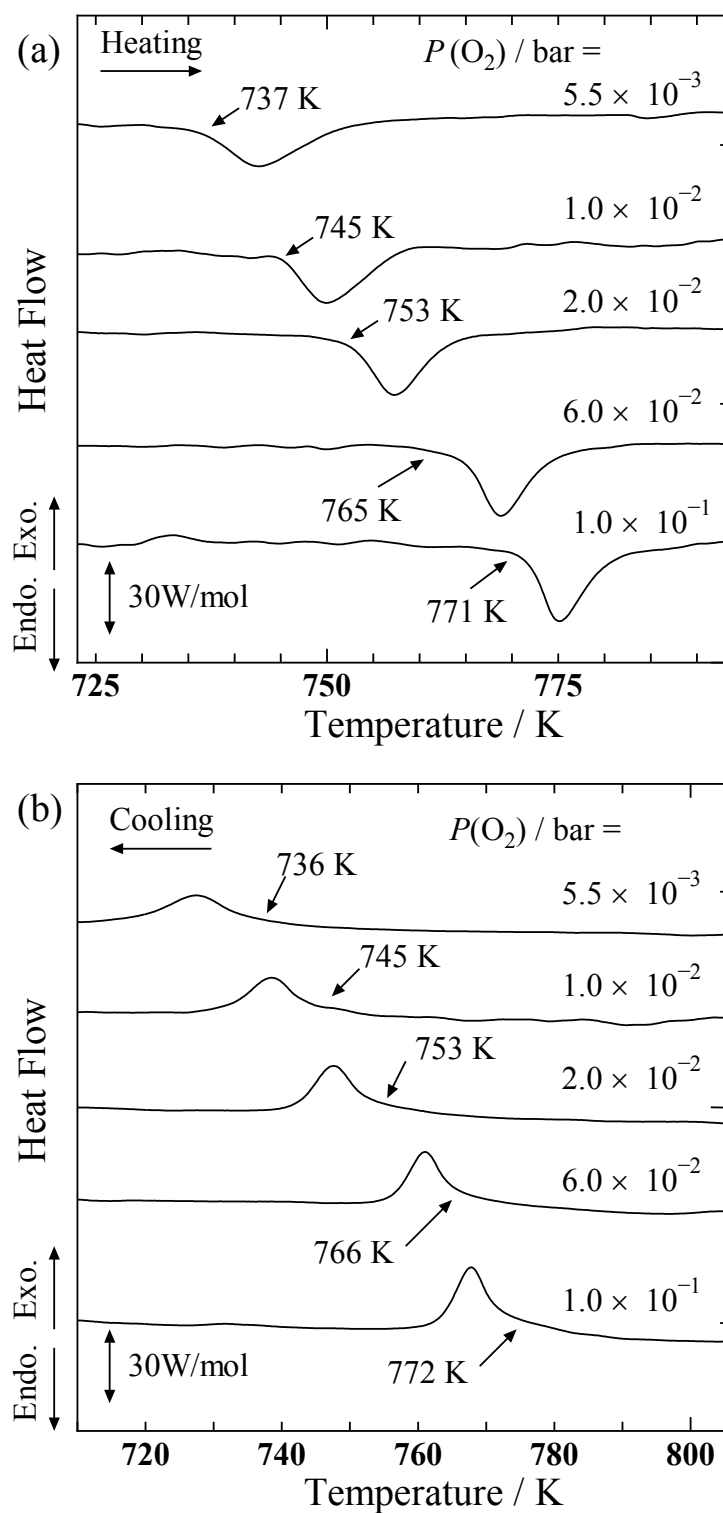
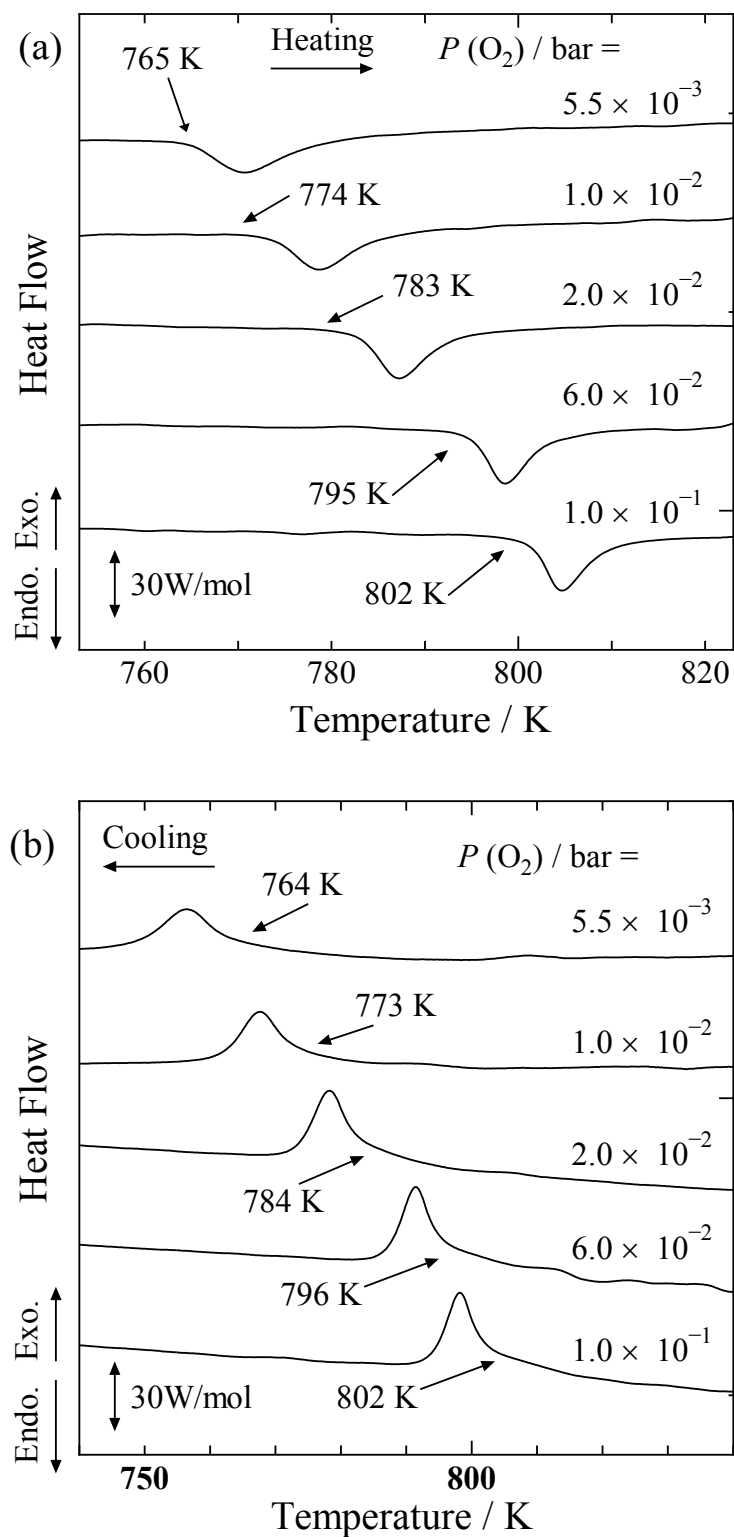
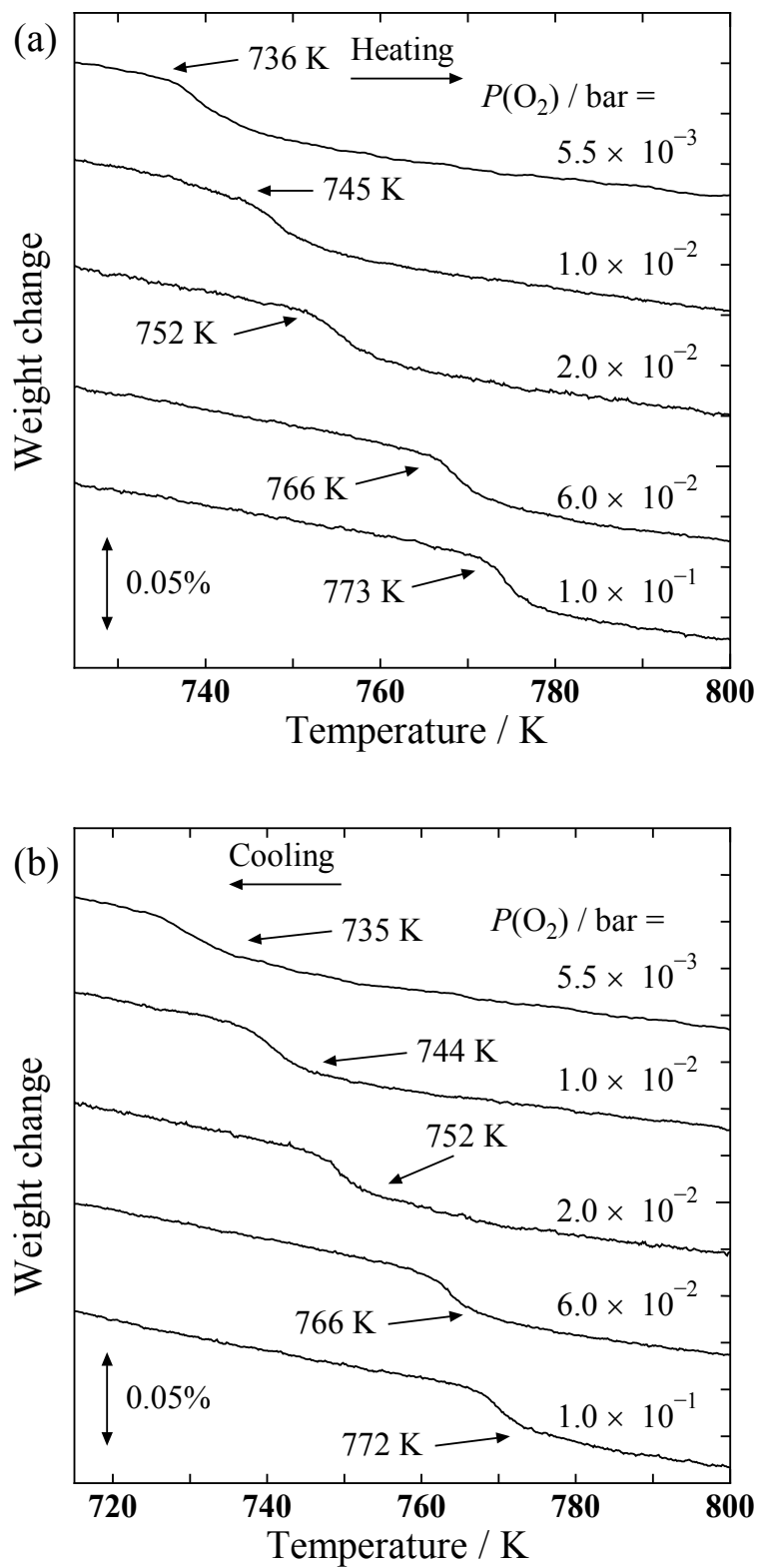


Figure S2. DSC curves of  $\text{PrNdNiO}_{4+\delta}$  around the phase transition temperatures under various  $P(\text{O}_2)$  during (a) heating and (b) cooling.



**Figure S3. DSC curves of  $\text{Pr}_{0.5}\text{Nd}_{1.5}\text{NiO}_{4+\delta}$  around the phase transition temperatures under various  $P(\text{O}_2)$  during (a) heating and (b) cooling.**



**Figure S4.** TG curves of PrNdNiO<sub>4+δ</sub> around the phase transition temperatures under various  $P(\text{O}_2)$  during (a) heating and (b) cooling.

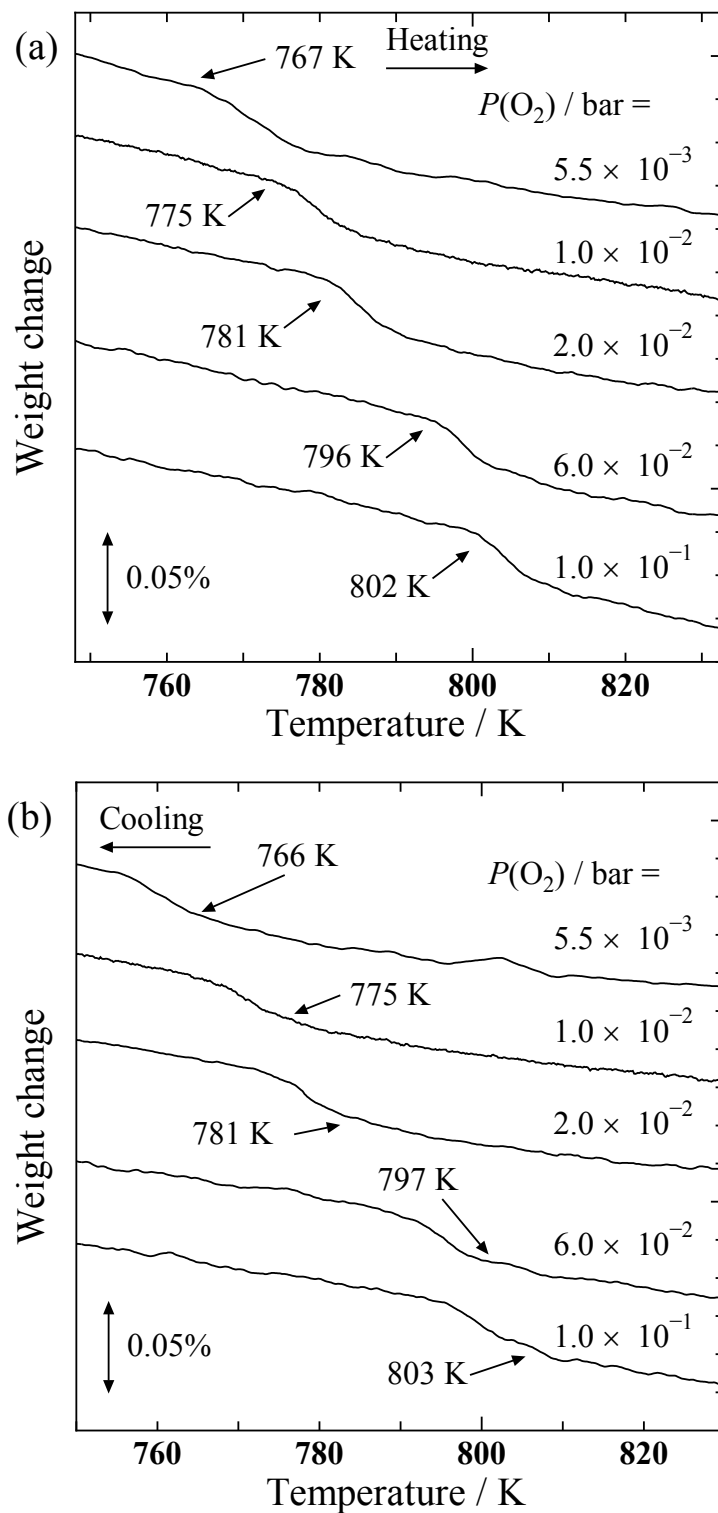


**Figure S5. TG curves of  $\text{Pr}_{0.5}\text{Nd}_{1.5}\text{NiO}_{4+\delta}$  around the phase transition temperatures under various  $P(\text{O}_2)$  during (a) heating and (b) cooling.**

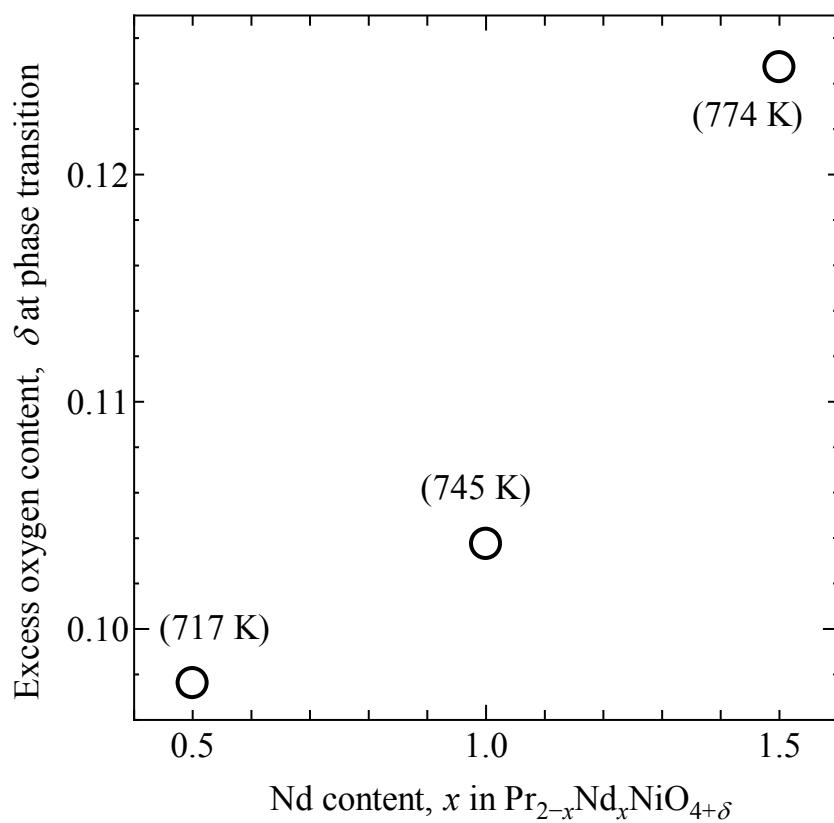


**Figure S6.** Compositional dependence of oxygen content,  $\delta$ , of  $\text{Pr}_{2-x}\text{Nd}_x\text{NiO}_{4+\delta}$  at the beginning of the phase transition during heating under  $P(\text{O}_2)$  of  $1.0 \times 10^{-2}$  bar. The values in parentheses show the phase transition temperatures.

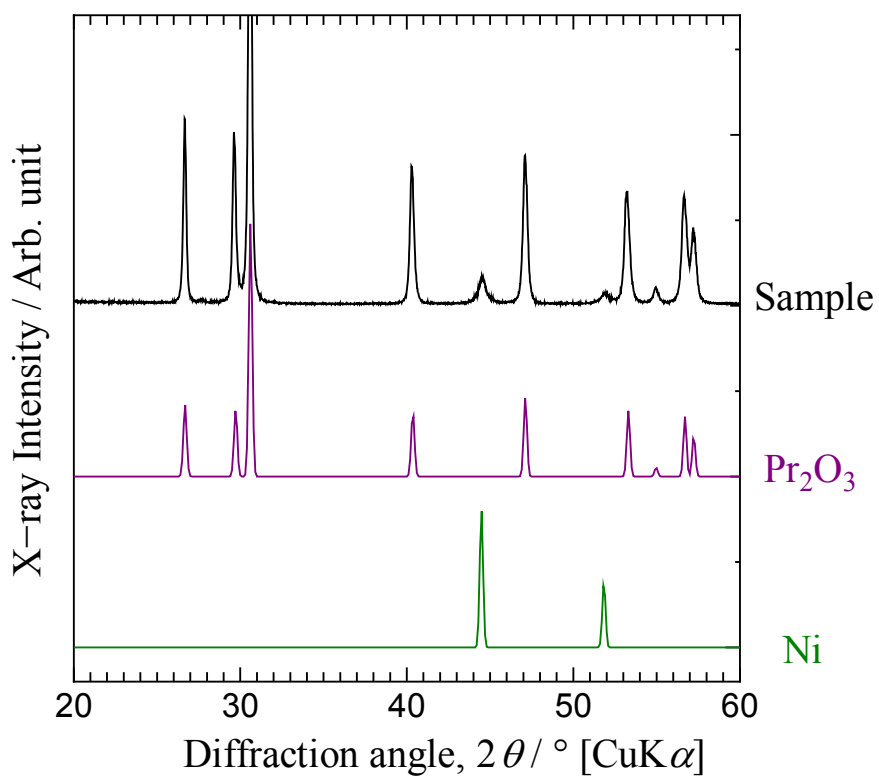


**Figure S7.** XRD pattern of  $\text{Pr}_2\text{NiO}_{4+\delta}$  after the decomposition reaction under  $2\% \text{H}_2/\text{N}_2$ . For reference, XRD patterns of  $\text{Pr}_2\text{O}_3$  and Ni are also shown in this figure [3, 4].

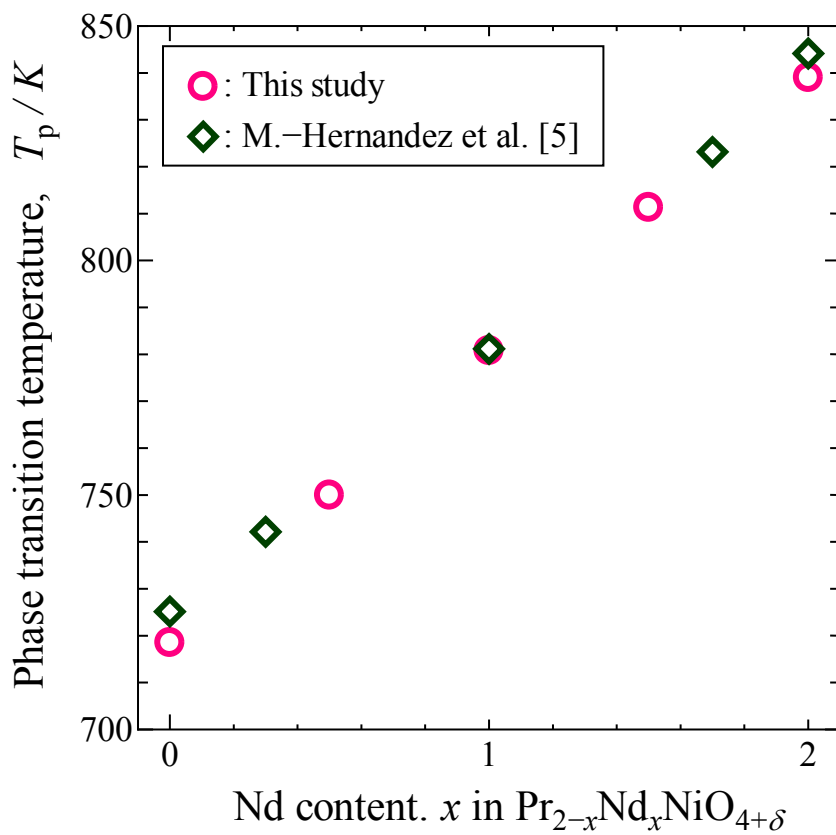


**Figure S8.** Compositional dependence of the phase transition temperatures,  $T_p$ , of  $\text{Pr}_{2-x}\text{Nd}_x\text{NiO}_{4+\delta}$  in air ( $P(\text{O}_2) = 0.205$  bar), estimated using  $\Delta S^\circ$  and  $\Delta H^\circ$  obtained in this work and measured with DTA [5].

**Table S1 (a) Lattice constants and (b) reliability factors for the XRD data of Pr<sub>2</sub>NiO<sub>4+δ</sub> by the Rietveld analysis with two kinds of models; a single phase of the orthorhombic *Fmmm* (Model 1) and the mixed phase of *Fmmm* and *F122/m* (Model 2), as shown in Figures S1 (a) and (b).**

**(a) Lattice constants**

Model	(Space group)	<i>a</i> / Å	<i>b</i> / Å	<i>c</i> / Å	<i>β</i> / °
Model 1	<i>Fmmm</i>	5.4005(22)	5.4612(23)	12.4581(51)	90
Model 2	<i>Fmmm</i>	5.4005(22)	5.4612(23)	12.4581(51)	90
	<i>F122/m</i>	5.14(49)	5.25(45)	12.45(31)	90.067(9)

**(b) Reliability factors**

Mode	(Space group)	<i>R</i> <sub>wp</sub>	<i>R</i> <sub>B</sub>	<i>R</i> <sub>F</sub>
Model 1	<i>Fmmm</i>	0.1724	0.0561	0.0362
Model 2	<i>Fmmm</i>	0.1713	0.0510	0.0285
	<i>F122/m</i>	0.1713	0.0362	0.0192

References

- [1] R. Oishi, M. Yoneyama, Y. Nishimaki, S. Torii, A. Hoshikawa, T. Ishigaki, T. Morishima, K. Mori, T. Kamiyama, Rietveld Analysis Software for J-PARC. *Nucl. Instrum. Meth. Phys. Res. A*, 2009, **600**, 94.
- [2] R. Oishi-Tomiyasu, M. Yonemura, T. Morishima, A. Hoshikawa, S. Torii, T. Ishigaki, T. Kamiyama, Application of Matrix Decomposition Algorithms for Singular Matrices to the Pawley Method for Z-Rietveld. *J. Appl. Cryst.*, 2012, **45**, 299.
- [3] H. C. R. Wolf, R. Hoppe, Eine Notiz Zum A-Typ der lanthanoidooxide: Über Pr<sub>2</sub>O<sub>3</sub>, *ZAAC*, 1985, **529**, 61.
- [4] J. Rouquette, J. Haines, G. Frayssé, A. Al-Zein, V. Bornard, M. Pintard, Ph. Papet, S. Hull, F. A. Gorelli, *Inorg. Chem.*, 2008, **47** [21], 9898.
- [5] A. M. Hernández, J. V. Castillo, A. Caneiro and L. Moggi, *J. Solid State Chem.*, 2019, **276**, 201.